17th Brazilian Congress of Thermal Sciences and Engineering
November 25th-28th, 2018, Águas de Lindóia, SP, Brazil

LAGRANGIAN VORTEX METHOD WITH IMPROVED BOUNDARY CONDITIONS TO STUDY THE AERODYNAMICS OF BLUFF BODY CLOSE TO A MOVING GROUND USING LAGRANGIAN LARGE EDDY SIMULATION

Crystianne Lilian de Andrade
Mechanical Engineering Institute, Federal University of Itajubá (UNIFEI), Itajubá, Brazil
crystiannelilian@yahoo.com.br

Luiz Antonio Alcântara Pereira
Mechanical Engineering Institute, Federal University of Itajubá (UNIFEI), Itajubá, Brazil
luizantp@unifei.edu.br

Alex Mendonça Bimbato
Department of Energy, São Paulo State University (UNESP), Guaratinguetá, Brazil
alexbimbato@feg.unesp.br

Abstract. *This numerical study is related to the determination of aerodynamic loads of a circular cylinder near a moving ground by using a two-dimensional purely Lagrangian vortex method. The purpose of this paper is to discuss a numerical techniques to impose improved boundary conditions on solid walls, and then reduce the time spend to satisfy the boundary conditions on solid walls. The body surface is discretized into M small straight panels. At each time step of the simulation, M new nascent Lamb-Oseen vortices are created a small distance ε off the body surface, just above of the panel control points, and M new sources with constant density are created on the M panels. The strengths of these new vortices elements and sources distributions are determined by imposing the no-slip and the impermeability conditions respectively. Two additional equations are necessary to ensure global circulation and mass conservation. The procedure above described yields in two different kind of algebraic systems to be solved independently. The flow past a circular cylinder in the subcritical flow regime ($Re = 1.0 \cdot 10^5$) is simulated and the results obtained, using each kind of algebraic system, are compared with experimental results available in the literature to validate the two numerical techniques.*

Keywords: *Vortex Method, Moving Ground, Aerodynamic Loads, reduction of the computational cost, Lagrangian Description.*

1. INTRODUCTION

When a bluff body moves in close proximity to the ground, the plane boundary will have an influence on the flow close to the body. In this case, the pattern of flow depends, not just the Reynolds number, but also on the gap-ratio *h/d* (*d* is cylinder diameter), where h is the gap between the cylinder and the ground. A well kwon practical example in engineering application is the flow around a motor car; the calculation of such flows is very complex because of the large separated regions and the additional ground effect.

The relative motion between body and ground was usually neglected in experimental investigations; Roshko et al. (1975) studied the fundamental effects of the gap-ratio but did not consider the relative motion between the body and the ground.

Nishino (2007) studied the aerodynamic behavior of a circular cylinder placed near a moving belt in a wind tunnel, where the velocity of the moving belt was the same as the oncoming flow. With that, the author concluded that there was practically no boundary layer developed on the ground. In his study the vortex shedding from a circular cylinder was investigated by visualizing air flows around it at Reynolds numbers of $4.0 \cdot 10^4 - 1.0 \cdot 10^5$. In order to inhibit the three-dimensional effects was used end-plates on the cylinder edges. Nishino (2007) classified the flow into three regimes: large-gap ($h/d > 0.5$), intermediate-gap ($0.35 < h/d < 0.5$), and small-gap ($h/d < 0.35$) regimes. In the large-gap regime, large-scale, kármán-type vortices were generated just behind the cylinder, resulting in higher values of C_D around 1.3. In contrast, in the small-gap regime, the large-scale vortex shedding totally ceased and instead a dead-fluid zone was created, bounded by two nearly parallel shear layers each producing only small-scale vortices in the near wake region. No substantial effect of *h/d* was observed in this regime: C_D was almost constant at a lower value of about 0.95. In the intermediate-gap regime, the kármán-type vortex shedding was found to be intermittent, i.e., typical instantaneous wake

patterns of both the large and small-gap regimes were intermittently observed, and C_D rapidly decreased as *h/d* decreased from 0.5 to 0.35.

Follow the conclusion of Nishino (2007), that if the ground runs at the same velocity of the incoming flow, there is practically no development of boundary layer, Bimbato et al. (2009) developed a numerical approach that uses a fixed ground, where is necessary to impose only the impermeability condition. As consequence, only on the body surface, near the ground plane, vortices are shedding in order to ensure the no-slip condition. On the other hand, on the ground, only the impenetrability condition is satisfied and a linear system of algebraic equations for the unknown source strengths is formed.

The aim of the present work is to show the efficiency of the algorithm in decreasing the time of calculation of the adherence condition and the ability to predict the drag coefficient of the circular cylinder near the ground. For that, a stationary cylinder in the subcritical flow regime ($Re=10^5$) is simulated using a two-dimensional Lagrangian Vortex Method. The local turbulence effects are taking into account through a second order velocity structure function model adapted to a Lagrangian Vortex Method (Alcântara Pereira et al., 2002) together with the boxes structure model (Andrade et al., 2016), which accelerates this calculation. The mass and the global circulation are simultaneously conserved using a source panel method and generation of vortex elements along the body surface. The aerodynamic loads are calculated using an integral formulation derived from the pressure Poisson equation (Shintani & Akamatsu, 1994).

The idea of the technique used here is to take into account the vortex strengths and the source strengths in the same linear system of algebraic to ensure the no-slip condition and the impenetrability condition at once. Therefore, in this paper are compared two versions of a Lagrangian vortex method implementation to simulate the two-dimensional, incompressible, unsteady flow around a circular cylinder in moving ground effect at a high Reynolds number: the one proposed by Bimbato et al. (2009) and with this new technique.

2. MATHEMATICAL FORMULATION

Figure 1 presents schematically the two-dimensional unsteady and incompressible flow of a Newtonian fluid with constant properties. As one can see, a circular cylinder is placed near a plane surface (ground), which has the same speed as the oncoming flow. The incident flow is given by U, and the semi-infinite fluid domain by $\Omega = S_1 \cup S_2 \cup S_3$, where S_1 is the body surface, S_2 is the plane surface and S_3 is the surface defined far from the body.

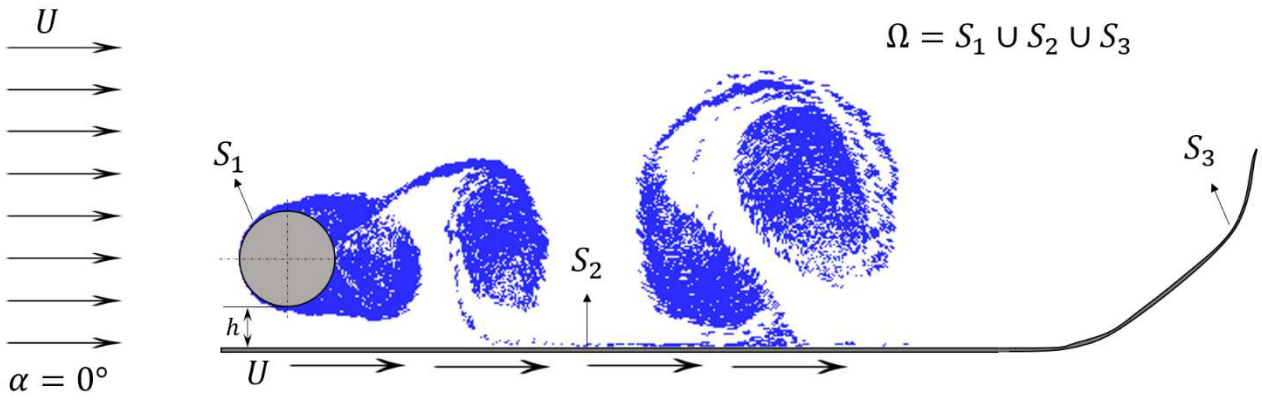

Figure 1. Definition of the fluid region

The problem is governed by the Navier-Stokes equations, which can be written in the form:

$$\frac{\partial \bar{u}_i}{\partial x_i} = 0, \tag{1}$$

$$\frac{\partial \bar{u}_i}{\partial t} + \bar{u}_i \frac{\partial}{\partial x_i}\bar{u}_j = -\frac{1}{\rho}\frac{\partial}{\partial x_i}\bar{p} + 2\frac{\partial}{\partial x_j}\left[(\nu + \nu_t)\bar{S}_{ij}\right], \tag{2}$$

where $\bar{u}_i$ is the velocity filtered field or the macro-scale field (Smagorinsky, 1963), $\bar{p}$ is the pressure filtered field, ρ is the density, ν is the molecular viscosity coefficient, ν_t is the eddy viscosity coefficient and $\bar{S}_{ij}$ is the deformation tensor of the filtered field given by Eq. (3).

$$\bar{S}_{ij} = \frac{1}{2}\left(\frac{\partial \bar{u}_i}{\partial x_j} + \frac{\partial \bar{u}_j}{\partial x_i}\right) \tag{3}$$

Métais and Lesieur (1992) considered that the small scales may not be too far from isotropic and proposed to use the local kinetic-energy spectrum E_{k_c} at the cut-off wave number (k_c) to define the eddy viscosity, ν_t.

Using a relation given by Batchelor (1953), Lesieur and Métais (1996) proposed to calculate the local spectrum at k_c with a second-order velocity structure function $\bar{F}_2$ of the filtered field:

$$\bar{F}_2(\boldsymbol{x}, \Delta^+, t) = \|\bar{\boldsymbol{u}}(\boldsymbol{x}, t) - \bar{\boldsymbol{u}}(\boldsymbol{x} + \boldsymbol{r}, t)\|^2_{|\boldsymbol{r}|=\Delta^+}. \tag{4}$$

From the Kolmogorov spectrum, the eddy viscosity can be written as a function of $\bar{F}_2$:

$$\nu_\mathrm{t} = 0.105 C_k^{-3/2} \Delta^+ \sqrt{\bar{F}_2(\boldsymbol{x}, \Delta^+, t)}, \tag{5}$$

where $C_k = 1.4$ is the Kolmogorov constant. In Eq. (4) is important to note that in three-dimensions the "average operator" is applied in the velocities $\bar{\boldsymbol{u}}(\boldsymbol{x} + \boldsymbol{r}, t)$ calculated under the surface of a sphere with the center in $\boldsymbol{x}$ and radius $|\boldsymbol{r}|$.

With the Navier-Stokes equations and the method to simulate the micro-scales, it is necessary to impose the boundary conditions. This is the adherence condition, which is divided in: (a) The impenetrability condition, which demands that the normal velocity component of the fluid particle $(\bar{u}_n)$ should be equal to the normal velocities components of the surfaces S_1 and S_2 (v_n) (Eq. (6)); (b) The no-slip condition which demands that the tangential velocity component of the fluid particle $(\bar{u}_\tau)$ should be equal to the tangential velocity component of the surfaces S_1 and S_2 (v_τ), (Eq. (7));

$$\bar{u}_n - v_n = 0, \text{ on } S_1 \text{ and } S_2, \tag{16}$$

$$\bar{u}_\tau - v_\tau = 0, \text{ on } S_1 \text{ and } S_2 \tag{17}$$

Therefore, the approach of this work is to simulate the phenomena that occur in the macro-scales by using the Navier-Stokes equations, Eq. (1) and Eq. (2), and the phenomena that occur in the micro-scales through the eddy viscosity coefficient (ν_t). For simulation of the Navier-Stokes equations, the present study uses Lagrangian Vortex Method that simulates the vorticity dynamic. The next section more detail about this method is given.

3. PRELIMINARY RESULTS

3.1. Flow around an isolated circular cylinder

The first step to validate the code was to simulate the flow around a stationary circular cylinder. This is a classical problem in fluid mechanics so it is a great starting point to validate the code. To obtain the result shown is Tab. 1, the same numerical parameter used by Bimbato (2012) were employed here: number of source flat panels used to represent the cylinder surface $(NP = 300)$, time increment $(\Delta t = 0.05)$ and the Lamb vortex core $(\sigma_0 = 0.001d)$. All the aerodynamic loads computations were evaluated between $10 \leq t \leq 75$, and the Reynolds number studied was 1.0×10^5.

As defined, the frequency of the detachment of vortices is measured by the Strouhal number defined as $St = fd/U$, being f the detachment frequency of vortices structures.

As can be seen in Table 1, the present numerical results agree very well with the experimental ones obtained by Blevins (1984), which have an uncertainty of about ±10%. Also for that case, the time-averaged lift coefficient, although very small, is not zero which is due to numerical approximations. It can be seen that there is no loss of information with the acceleration performed in the structure of satisfying the boundary condition since the results present by Bimbato (2012) disagree only in 3.19%, which can be due to accumulated truncation or rounding errors in the calculation process.

Table 1. Mean values of drag and lift coefficients and Strouhal number for an isolated circular cylinder ($Re = 10^5$)

Authors	$\bar{C}_D$	$\bar{C}_L$	$\bar{St}$
Blevins (1984)	1.20	-	0.19
Bimbato (2012)	1.22	0.021	0.21
Present result	1.18	0.020	0.21

In Figure 5, the vortex shedding period can be seen in oscillations of the lift and drag coefficients. As found in the characteristic of an isolated circular, the drag coefficient oscillates two times more than the lift coefficient. This means

that for each vortex structure detachment, the lift coefficient completes a period, while the drag coefficient completes two periods.

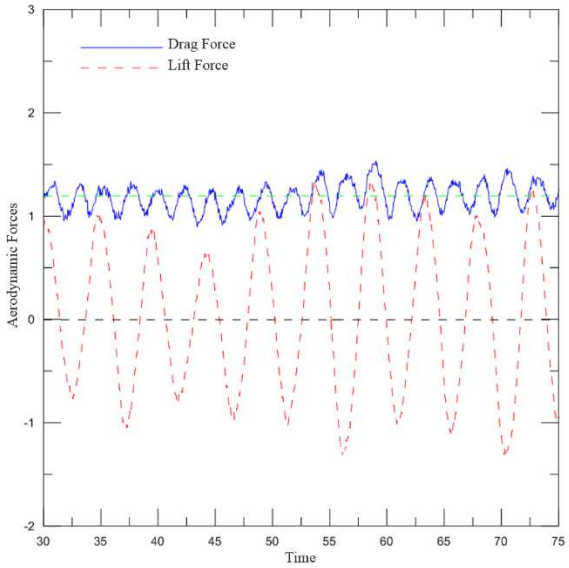

Figure 5. Time evolution of the aerodynamic forces for the isolated circular cylinder ($Re = 10^5$).

As the code is able to simulate flow around an isolated circular cylinder, we pass to the next step, which is to validate the code for the simulation of the ground effect phenomenon, and to predict the aerodynamic forces on circular cylinder. In the simulations made in order to study the ground effect, the numerical parameters used in the isolated circular cylinder case were maintained, and the moving ground surface was represented by $NP_2 = 200$ sources flat panels. It is necessary to point out that the same numerical parameters used by Bimbato (2012) employed here, as we want to compare with his work, which were successfully validated.

3.2. Circular cylinder in ground effect

In order to validate the numerical technique to satisfy the boundary condition, here we compared the present results with those present by Bimbato (2012), which were successfully validated by using the Lagrangian Vortex Method. We also compared the present results with the approximately two-dimensional experimental ones obtained Nishino (2007). In his experimental study, Nishino (2007) shows the influence of the tip effect on the aerodynamic behavior of the body, and in order to study the approximately two-dimensional flow, the author fixed end-plates on the cylinder extremities (Fig. 6). The configuration $y_e/d = 0.4$ (where y_e is the distance between the edge of the end-plate and the edge of the circular cylinder) represents the configuration in which the flow is closer to a 2-D configuration. Thus, we mainly compare the numerical results of the present work with the experimental ones obtained by Nishino (2007) with this configuration.

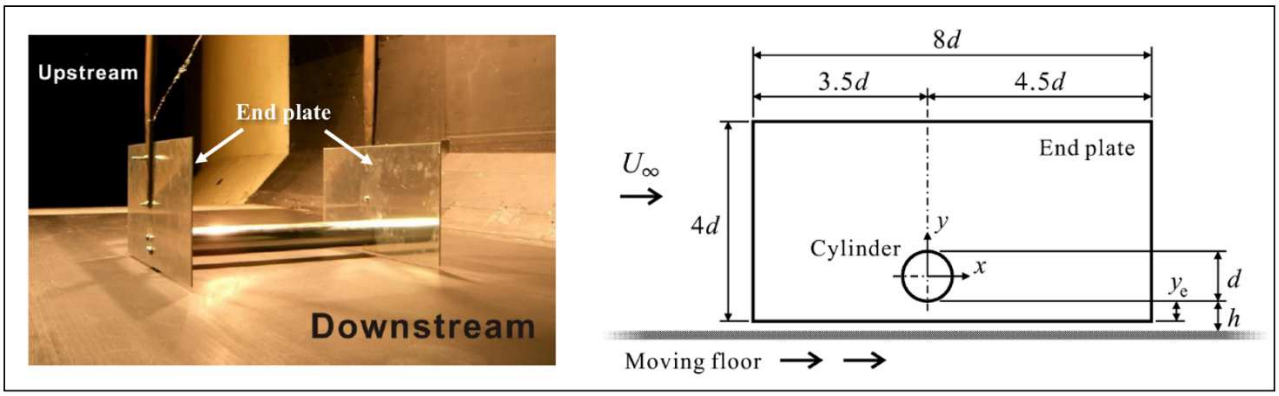

Figure 6. Experimental apparatus used in wind tunnel tests (adapted from Nishino, 2007).

In Figure 7 is shown the variation of the mean drag coefficients with h/d presented by Zdravkovich (2003), Nishino (2007), Bimbato et al. (2012a, b) and the present simulation. In all this work the ground moves with the same velocity of the incident flow. From Figure 7, one can check that:

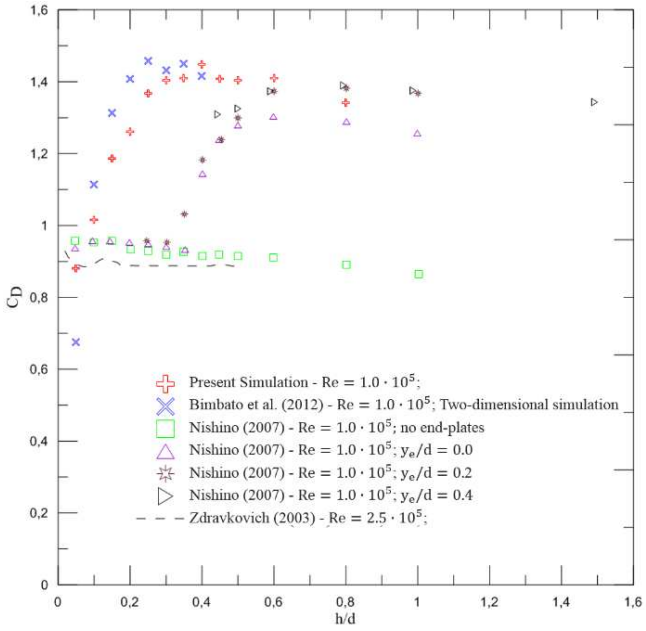

Figure 7. Comparison between the results obtained for the average drag coefficient for the circular cylinder subjected to the ground effect.

(a) Firstly, as discussed by Nishino (2007), one of the mechanisms that govern the phenomenon of the ground effect is related to the three-dimensionality of the flow. Thus, as can be observed in the experiments in which the three-dimensional effects were important, the drag coefficient increases smoothly as the circular cylinder come close to the ground. In the other hand, in the case where the flow is approximately two dimensional ($y_e/d = 0.0$, 0.2 and 0.4), there was a rapid reduction in the coefficient of drag with the decrease of h/d to less than 0.5 which also occurred with the present simulation;

(b) Comparing the results of the present simulation with those presented by Nishino (2007), it is verified that the higher the value of y_e/d, the smaller the difference between the presented values. This highlights that the larger the distance between the edge of the end-plates and the edge of the circular cylinder, the greater the efficiency of it in inhibiting the three-dimensional effects. It can be seen that for $h/d \geq 0.45$, the results of the present simulation differ from the experimental ones by 8% on average, which is acceptable for numerical simulations. For distances $h/d \leq 0.40$, the difference between the experimental and numerical results increases. However, as the end-plates must not touch the ground, y_e/d decreases and, as well as the effectiveness of the end-plates in producing two-dimensional flow, justifying the increase in the difference between the results.

(c) It is verified that the results presented in the present simulation and those presented by Bimbato et al. (2012a, b) differentiate, on average, 6% from each other. However, there are cases, such as $h/d = 0.4$, where the results differ by 2%. This is due to numerical calculations and rounding.

To explain this mechanism of shedding vortex near a moving ground, a more detailed analysis is made of the flow around the circular cylinder at a distance of 0.45 from the ground ($h/d = 0.45$). This gap ratio is chosen as it is possible to compare the results of the present simulation with the one made by Nishino (2007) where the end-plates have the best efficiency to produce two-dimensional flow. In Table 2 the average values of the drag and lift coefficients and the Strouhal number for this case are presented. It is observed that the result obtained for the drag coefficient in the present simulation differs by approximately 4.6% in relation to the result presented by Bimbato (2012) and 7.32% in relation to the experimental result presented by Nishino (2007). The discrepancy with respect to the experimental result is acceptable since even using the end-plates, the flow is not perfectly two-dimensional.

Table 2. Mean values of drag and lift coefficients and Strouhal number for a circular cylinder near the ground ($Re = 10^5$ and $h/d = 0.45$)

Authors	$\bar{C}_D$	$\bar{C}_L$	$\bar{St}$
Nishino (2007) – $y_e/d = 0.4$	1.311	0.102	-
Bimbato (2012)	1.474	0.154	0.205
Present result	1.407	0.003	0.200

For that case, time-averaged pressure coefficient and the temporal series of drag and lift coefficients on the circular cylinder are presented in Figure 8. The time-average pressure distribution on the surface for the simulation of the isolated circular cylinder is also shown in Figure 8 (a). Comparing the two curves in Fig. 8 (a) it is possible to verify that the pressure at the back of the circular cylinder under the ground effect is smaller than in the case of the isolated cylinder, which justifies the increase of the drag coefficient of 1,184 (isolated circular cylinder) to 1,407.

Comparing now the curves representing the evolution of aerodynamic forces for the case of the isolated circular cylinder (fig. 5) and for the case of the circular cylinder under the ground effect (Fig. 8 (a)), it can be seen that, unlike the first case, for the cylinder under the ground effect, in a period of oscillation of the drag coefficient, there is an amplitude of higher peak and another smaller. This occurs due to the blocking effect imposed by the ground presence, which is one of the mechanisms that govern the ground effect phenomenon.

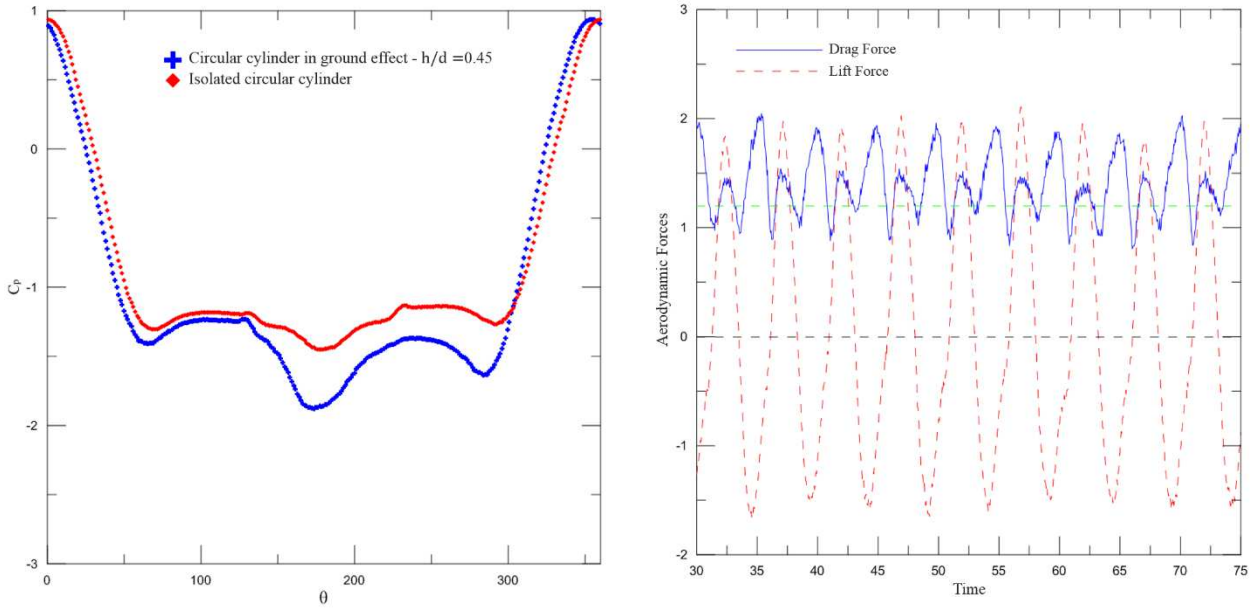

(a) time-averaged pressure coefficient. (b) temporal series of drag and lift coefficients

Figure 8. Aerodynamic loads acting on a circular cylinder in ground effect ($Re = 10^5$ and $h/d = 0.45$).

This effect causes the anticlockwise vortex (lower) to have its development limited by the presence of the ground, while the clockwise vortex (upper) has complete freedom to develop until it is finally incorporated by the wake vortex. Thus, larger amplitude peaks are generated in the drag coefficient curve in the development of a upper vortex structure and smaller amplitude peaks in the development of an anticlockwise (lower) vortex structure (see fig. 9 (a)).

For the evolution of the lift coefficient (fig. 9 (b)), in general, the same dynamics of generation and detachment of vortex structures observed for the isolated circular cylinder is verified. At instant represented by point A in fig. 9 (b), there is a low-pressure distribution at upper cylinder surface due to the growing of a vortex structure near the cylinder, which is at an initial stage of development. This explains the maximum lift force in that moment. The upper clockwise vortex structure continues growing fed by the vorticity of the boundary layer to which it is connected.

At instant represented by point *B*, the lower vortex structure, which is larger than that the opposite side, attracts the upper vortex, which cuts off the vorticity supply of the lower one, causing it to shed on the lower side of the cylinder, becoming a free vortex (see Fig. 9 (b)).

At instant represented by point *C*, an anticlockwise vortex structure, that was shed on the lower side of the cylinder at instant *B*, is on its initial stage of development. Therefore, there is a low-pressure distribution at lower cylinder surface, which explains the minimum lift force (Fig. 9 (b)). This structure grows and is attracted by the opposite shear layer which is feeding the clockwise vortex structure causing its detachment. That moment corresponds to the instant D.

Despite the similarity of the dynamics of generation and detachment of vortex structures in the isolated circular cylinder, it is possible to verify that under the ground effect the anticlockwise (lower) vortex structure develops closer to the body (figure 9 (b), point C) than in the isolated case. Thus, there is a lower pressure in the back of the body, which justifies the increase of the average drag coefficient in relation to the case in which the body is isolated.

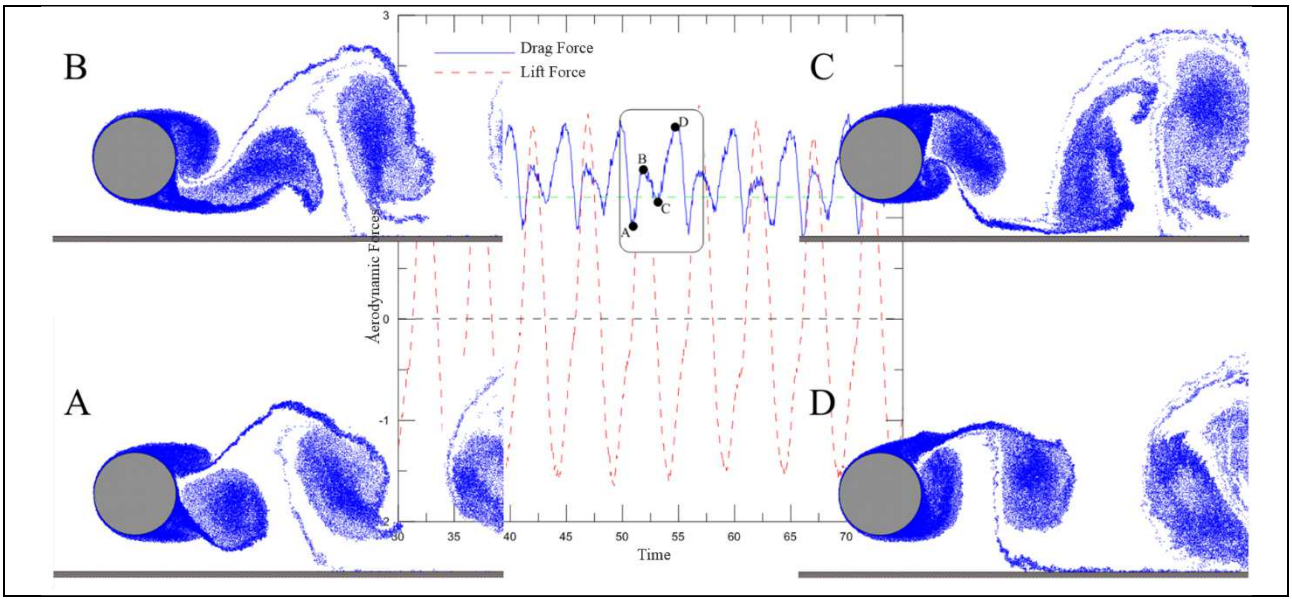

(a) In the period of the drag coefficient

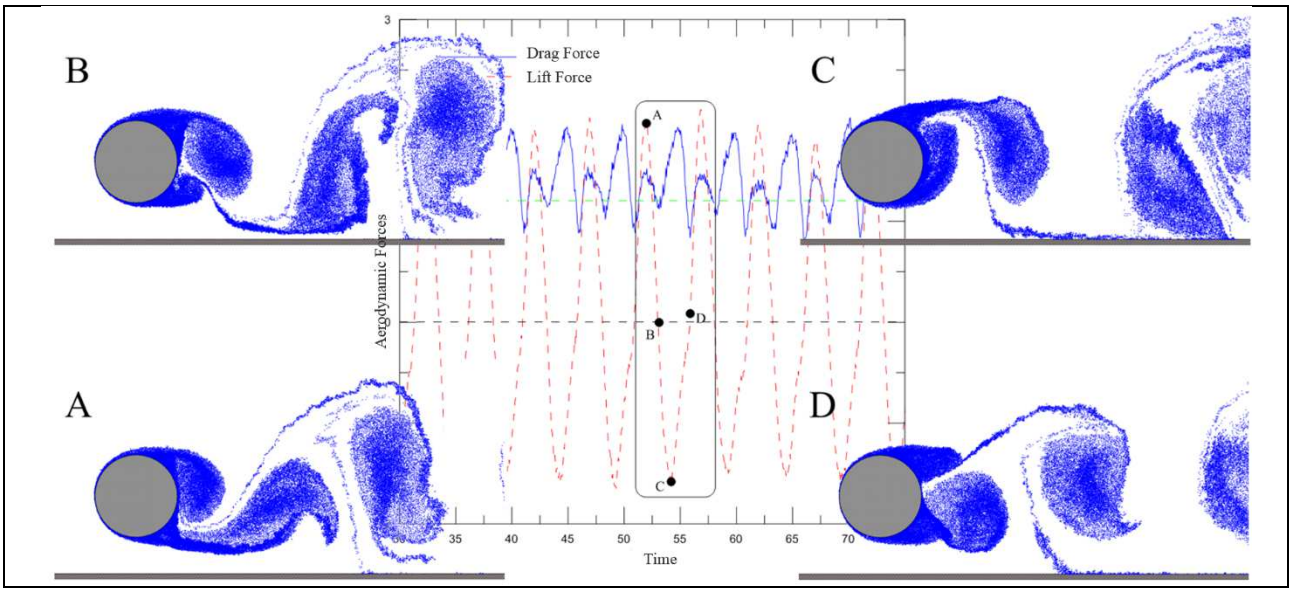

(b) In the period of the lift coefficient

Figure 9. Temporal series for the near wake structures for the flow past a circular cyinder in the ground effect ($Re = 10^5$).

The most important point here is to show that the technique applies here to compute the boundary condition effectively decrease the simulated time. Bimbato (2012) state that the simulations presented in his work had a duration of 584h (approximately 25 days) in a computer with the following configuration: INTEL CORE I7 - 2.8GHZ (BOX) 8MB CACHE (i7-860), MB INTEL DH55TC, 8GB RAM DDR3 1333 MHZ. The author simulates until $t = 75.0$, reaching a wake vortex with 450,000 vortices. Using a computer with the same configuration, reaching a wake vortex with the same number of vortices at $t = 75.0$, this present simulation spent 294h (approximately 13 days), which represent about 50% of time consumed by Bimbato (2012). It is necessary to point out that about 51% of the decrease of the time spent in simulation is due to the new numerical technique used to compute the boundary condition. Thus, the decrease of the time

is also due to the box structure build to compute the eddy of viscosity to simulate the turbulence (for more detail see Andrade et al., 2016).

In conclusion, it is important to see that present program is able to simulate numerically the flow around a circular cylinder near the ground more efficiently, which mean in a smaller computational cost.

6. ACKNOWLEDGEMENTS

This study was supported by FAPEMIG (Proc. APQ-02175-14).

7. REFERENCES

Alcântara Pereira, L. A., Ricci, J. E. R., Hirata, M. H., Silveira Neto, A., 2002, "Simulation of the Vortex-Shedding Flow about a Circular Cylinder with Turbulence Modeling", CFD Journal, Vol. 11, No. 3, october, pp. 315-322.

Andrade, C. L.; Pereira, L. A. A.; Bimbato, A. M.. "Boxes Structure Construction around the Clusters of Vortex Elements to Reduce the Computational Cost of a Lagrangian Vortex Method with Roughness Model". 16th Brazilian Congress of Thermal Sciences and Engineering, 2016, Vitória. Proceedings of ENCIT 2016, 2016.

Batchelor, G. K., 1953, "The Theory of Homogeneous Turbulence", Cambridge University Press.

Bimbato, A. M., Alcântara Pereira, L. A., Hirata, M. H., 2009, "Simulation of Viscous Flow around a Circular Cylinder near a Moving Ground", J. of the Braz. Soc. of Mech. Sci. & Eng., Vol. XXXI, No. 3, pp. 243-252.

Bimbato, A. M., 2012. "Study of Turbulent Flows around a Smooth or a Rough Bluff Body Using the Discrete Vortex Method". D.Sc. Thesis, Institute of Mechanical Engineering, UNIFEI, Itajubá, MG, Brazil (in Portuguese).

Bimbato, A. M., Alcântara Pereira, L. A., Hirata, M. H. (2012a), "Corrected Lagrangian LES Model for Vortex Method", In Proceedings of the EPTT 2012 8th Spring School on Transition and Turbulence. São Paulo, SP, Brazil.

Bimbato, A. M., Alcântara Pereira, L. A., Hirata, M. H. (2012b), "Vortex shedding suppression on a bluff body in the vicinity of a moving ground", 14th Brazilian Congress of Thermal Sciences and Engineering October 18-22, 2012, Rio de Janeiro, RJ, Brazil.

Blevins, R. D., 1984, Applied Fluid Dynamics Handbook, Van Nostrand Reinhold, Co.

Lesieur, M. and Métais, O., 1996, "New trends in large-eddy simulation of turbulence". A Review in Fluid Mechanics, Vol. 28, pp. 45-82.

Métais, O. and Lesieur, M., 1992, "Spectral Large-Eddy Simulations of Isotropic and Stably-Statified Turbulence", J. Fluid Mech., 239, pp. 157-194.

Nishino, T., 2007, Dynamics and Stability of Flow Past a Circular Cylinder in Ground Effect, Ph.D. Thesis, Faculty of Engineering, Science and Mathematics, University of Southampton, 145p.

Roshko, A., Steinolfson, A. and Chattoorgoon, V., 1975, "Flow Forces on a Cylinder near a Wall or near another Cylinder", Proceedings of the 2nd U.S. National Conference on Wind Engineering Research, Fort Collins, Paper IV-15.

Shintani, M. and Akamatsu, T., 1994, "Investigation of Two Dimensional Discrete Vortex Method with Viscous Diffusion Model", Computational Fluid Dynamics Journal, Vol. 3, No. 2, pp. 237-254.

Smagorinsky, J., 1963, "General circulation experiments with the primitive equations", Mon. Weather Rev. 91,3,0099-164.

Zdravkovich, M. M., 2003, Flow around Circular Cylinders: Vol. 2: Applications, Oxford University Press, Oxford, UK.

8. RESPONSIBILITY NOTICE

The authors are the only responsible for the printed material included in this paper.